

Pattern Generation in Synthetic Aperture Lithography (SAL)

Berthold K. P. Horn — 2002 March 15

Synthetic Aperture Lithography (SAL) uses apparatus similar to that used in Synthetic Aperture Microscopy (SAM), as described by Mermelstein [1].

We wish to create patterns by interfering N beams of coherent light. The wavenumbers of the beams all lie on a circle in the frequency domain, typically equally spaced around the circle. If the wavelength of the monochromatic light is λ and the angle between the incident beams and the reference surface is θ , then the ring in the frequency domain has radius

$$\omega_0 = 2\pi/\lambda_0$$

where

$$\lambda_0 = \lambda/\cos\theta$$

is the effective wavelength on the surface. The equivalent numerical aperture is $\cos\theta$ (i.e., the sine of half the cone angle).

Using wavenumbers confined to a circle leads to interference patterns that are independent of height above the reference plane, since the difference of any two wavenumbers has zero component in the z direction (perpendicular to the reference plane). This gives us potentially infinite depth of field. The price we pay for this advantage is that the class of possible patterns we can create is limited.

Limitations on Patterns Generated

The N beams create $N(N - 1)/2$ pairwise interference patterns. Hence the N complex amplitudes of the beams affect $N(N - 1)/2$ contributions to the Fourier transform of the interference pattern. It is clear that there must be some limitations then on what patterns can be generated, beyond those mentioned above, since there are only $2N$ “controls” — namely the amplitudes and phases of the beams.

Linear Superposition Does Not Hold

The complex amplitudes of the electric fields of the beams add up at a given point, but the brightness does not, since it is the magnitude squared of the complex amplitude. As a result, superposition does not hold for brightness. This means that we cannot directly assemble complex patterns by adding up the complex amplitudes needed to create simpler patterns. At the same time, some remarkable patterns can result from the non-linear interaction of destructive and constructive interference.

Note that we can achieve superposition using successive exposures, although this is of course slower than putting down the desired pattern in one exposure. So we should attempt to get as as complex a pattern as possible in a single exposure in order to reduce the overall exposure time.

Approaching the Problem

There are at least two ways to make progress on this problem:

- (i) determine what patterns are generated by some simple mathematically defined complex amplitude distributions for the beams (forward problem); and
- (ii) use numerical optimization techniques to find complex amplitude distributions that produce a pattern that best fits a desired pattern (inverse problem).

As it turns out, one method can benefit from insights obtained from the other. The following discussion illustrates.

The Forward Problem

One approach to discovering useful beam amplitudes to generate particular patterns is to first study the “forward problem” of finding the pattern produced by particularly simple choices of complex amplitudes.

If the amplitude, phase, and polarization vector of beam l are A_l , ϕ_l , $\hat{\mathbf{p}}_l$ respectively, then the electric field at position \mathbf{r} at time t is

$$\mathbf{E}(\mathbf{r}, t) = \sum_{l=1}^N A_l \cos(\mathbf{k}_l \cdot \mathbf{r} - \omega_l t + \phi_l) \hat{\mathbf{p}}_l$$

If we assume that the frequencies ω_l of the beams are all the same, then the brightness averaged over one cycle ($T = 2\pi/\omega_l$) is given by

$$I(\mathbf{r}) = \frac{1}{2} \sum_{l=1}^N A_l^2 + \sum_{l=1}^{N-1} \sum_{m=l+1}^N A_l A_m \cos(\mathbf{k}_{lm} \cdot \mathbf{r} + \phi_{lm}) \hat{\mathbf{p}}_l \cdot \hat{\mathbf{p}}_m$$

where $\mathbf{k}_{lm} = \mathbf{k}_l - \mathbf{k}_m$ and $\phi_{lm} = \phi_l - \phi_m$.

Point of Light

We can produce a point of light at the origin if we arrange for all the beams to constructively interfere there. We can do this by adjusting all of the phases so they are zero at the origin. In the limit of an infinite number of beams on the circle, with the same amplitude on all beams, we are essentially taking the inverse Fourier transform of an impulsive ring of radius ω_0 . Using polar coordinates for spatial as well as frequency

coordinates, we have

$$f(r, \alpha) = \frac{1}{2\pi} \int_0^\infty \int_{-\pi}^\pi \frac{1}{\omega_0} \delta(\omega - \omega_0) e^{jr\omega \cos(\alpha - \phi)} \omega d\omega d\phi$$

or

$$f(r, \alpha) = \frac{1}{2\pi} \int_{-\pi}^\pi e^{jr\omega_0 \cos \phi} d\phi$$

So we find that the electric field is proportional to

$$J_0(\omega_0 r)$$

where r is the distance from the origin and J_0 is the Bessel function of the first kind of order zero. The brightness is just the square of the above expression.

If the beams all make the same angle θ with respect to the surface, then the interference pattern is constant in the direction perpendicular to the surface (because pairwise difference between wavenumbers, $\mathbf{k}_l - \mathbf{k}_m$, all have zero z -components). So the “point of light” is really a “line of light” when considered in three dimensions.

Lens of Equivalent NA

It is interesting to compare this to the pattern produced by a lens of the same numerical aperture, that is, where the rays from the edge of the lens make an angle θ with the surface. In this case the pattern is obtained by taking the inverse Fourier transform of a disc rather than just a ring. The disc can be treated as the superposition of an infinite number of rings of various radii. The amplitude of the pattern created is proportional to

$$\int_0^{\omega_0} \omega J_0(\omega r) d\omega$$

or, letting $\omega' = \omega r$,

$$\frac{1}{r^2} \int_0^{\omega_0 r} \omega' J_0(\omega') d\omega'$$

Using the identity

$$\frac{d}{dz} z J_1(z) = z J_0(z)$$

we finally find that the electric field is proportional to

$$2 \frac{J_1(\omega_0 r)}{(\omega_0 r)}$$

Again, the brightness is the square of this expression, which is the familiar “Airy disk” referred to in discussion of the limits of resolution of optical equipment with circular apertures. For the lens, the pattern is not constant in the direction perpendicular to the surface, having very limited depth of field if the numerical aperture is large.

Note that the first zero of $J_0(\omega_0 r)$ occurs at $\omega_0 r = 2.4048\dots$ while the first zero of $J_1(\omega_0 r)$ occurs only at $\omega_0 r = 3.8317\dots$. So the ring of beams produces a considerably smaller point (radius of about $0.382\dots\lambda_0$) than does a lens of equal NA (radius of about $0.609\dots\lambda_0$).

On the other hand, the “side lobes” decay only with $1/r$ when using the ring compared to $1/r^3$ for the lens. This is because

$$J_n(x) \approx \sqrt{\frac{2}{\pi x}} \cos\left(x - \frac{n\pi}{2} - \frac{\pi}{4}\right)$$

for $x \gg 1$. More of the energy is in the central disc with the lens than with the ring of beams.

Cyclical Variation of Phase

Suppose now that, instead of forcing all the beams to the same phase, we adjust the phase of each beam according to the rule $\phi = n\xi$ for some integer n , where ξ is the angle that the beam direction makes with the x -axis when projected onto the reference plane.

Now we have destructive interference at the origin and the complex amplitude there is zero. If we take the inverse Fourier transform of the ring with this phase component we find that the amplitude of the electric field is now

$$f(r, \alpha) = \frac{1}{2\pi} \int_{-\pi}^{\pi} e^{j(\omega_0 r \cos \phi - n\phi)} d\phi$$

so the electric field is proportional to

$$J_n(\omega_0 r)$$

The Bessel function of the first kind of order n , for $n > 0$, starts at zero for $r = 0$ and has its first maximum around

$$x(n) \approx n + \frac{2n + 1}{n + 3}$$

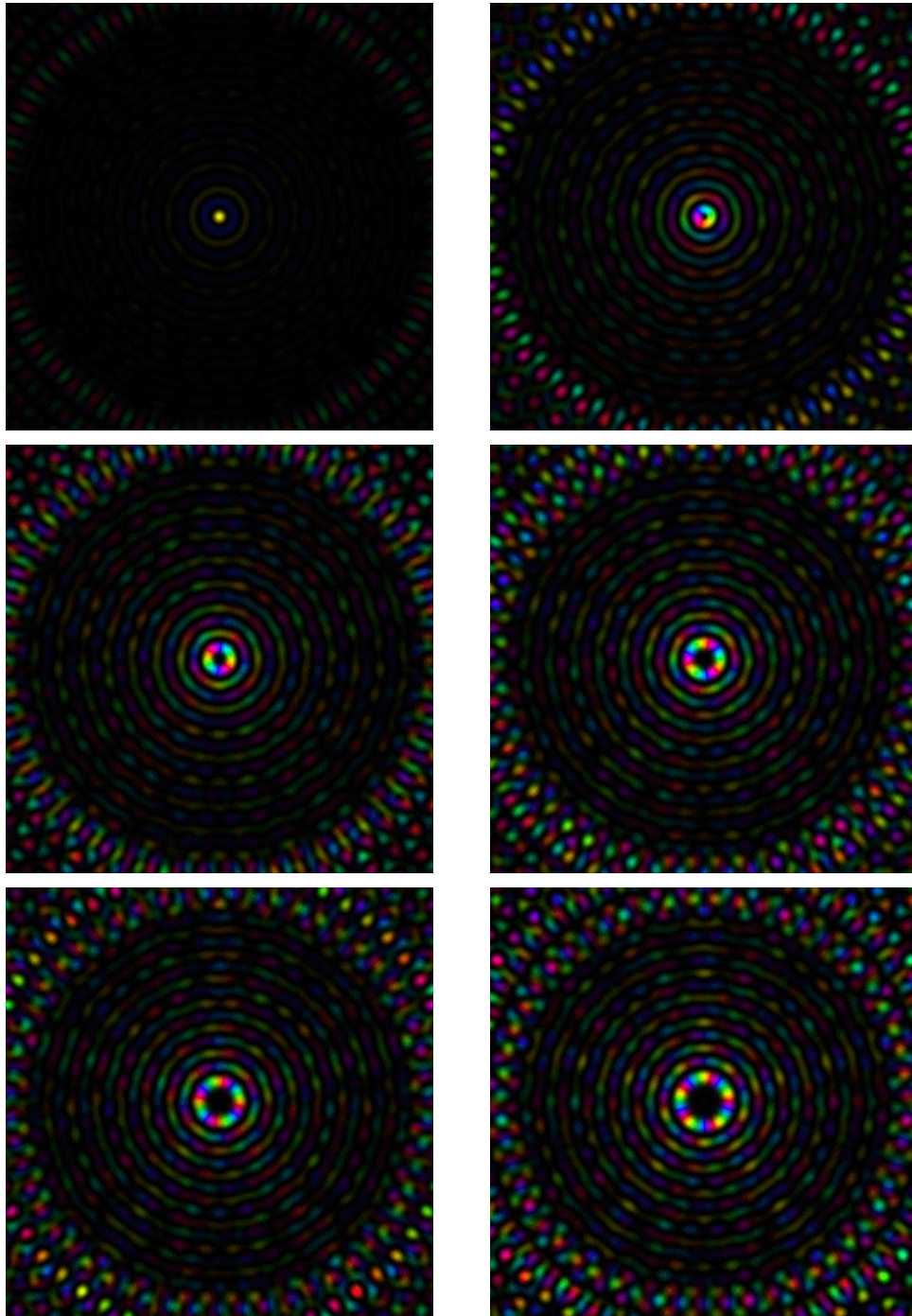
So a dark area at the origin of radius roughly $n\lambda_0/(2\pi)$ is surrounded by a ring of light of radius $x(n)\lambda_0/(2\pi)$, with additional “halos” further out.

The destructive interference in the center is remarkably good over a considerable area, since

$$J_n(x) \approx \frac{1}{n!} \left(\frac{x}{2}\right)^n$$

for $x \ll 1$.

While the ring may not be a pattern of direct interest in lithography, the above does suggest a way of delivering high power electromagnetic waves to a ring shaped area while “shielding” the interior of the ring with surprising effectiveness as the result of destructive interference there.



In the figures, brightness indicates amplitude, while color indicates phase. Shown are the bright rings for $n = 0, 1, \dots, 5$. Note (i) the dark interior of the ring, (ii) the secondary rings or “ghosts”, and (iii) the artifacts in the outer areas resulting from use of only a finite number of beams.

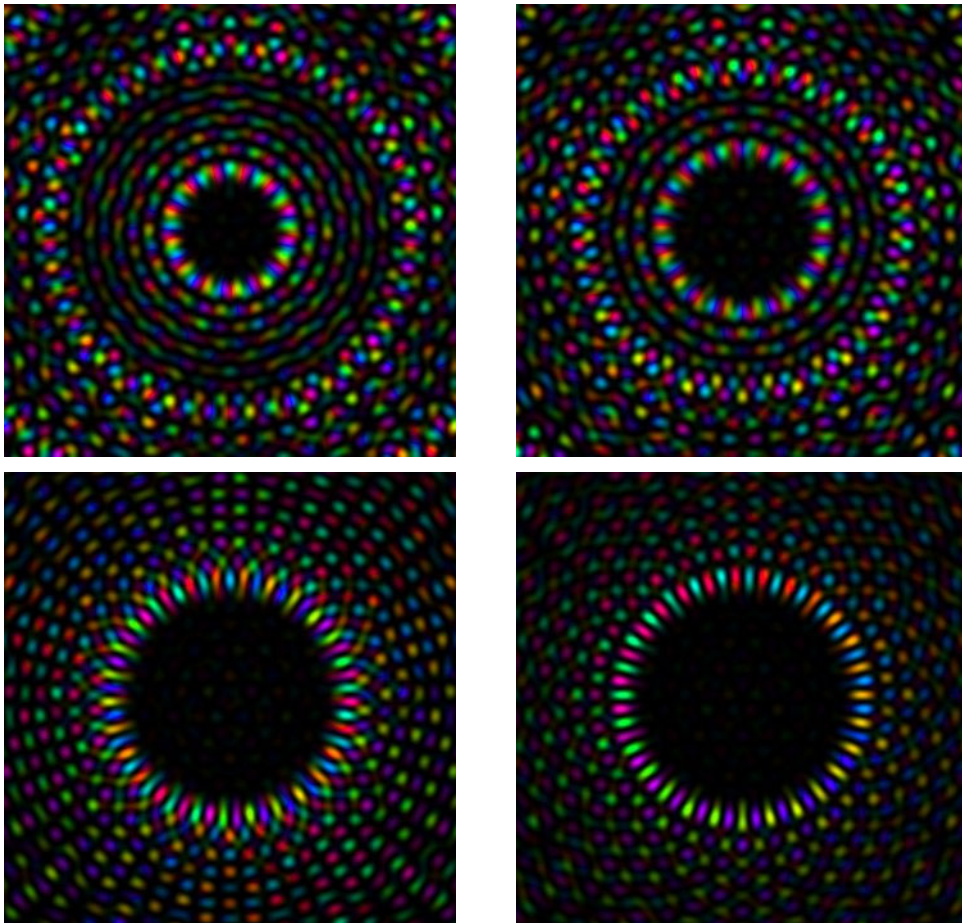
Artifacts due to Finite Number of Beams

If we use a finite number N of beams, then the pattern is very close to the above in areas near the origin, as long as $n \ll N$. The brightness along the ring is more or less constant, again, as long as $n \ll N$. Some artifact appear outside the ring at a radius of approximately

$$r_a \approx N/(2\pi)\lambda_0$$

This ring of artifact moves inwards as n is increased, to merge with the bright ring when $n = N/2$.

Note that due to aliasing we do not obtain new patterns when n is larger than $N/2$, since, the pattern for n , when $N/2 < n < N$, is the same as that for $n' = N - n$.



The patterns for n equal to 13, 18, 26 and 27 with $N = 55$ beams. The artifact ring moves inwards as n increases, to merge with the bright ring when $n = N/2$. When $n = N/2$, neighboring beams have opposite phase. The uniform bright ring breaks up into N bright spots as n increases.

Phase Variation Along the Bright Ring

In the limit of an infinite number of beams, the amplitude (and hence the brightness) is constant along the bright ring, but the phase is not. The symmetry of the arrangement should make it clear that the phase will vary along the bright ring, and it will go through $2\pi n$ radians when we go around the ring once.

Now along an ordinary travelling of wavelength λ_0 we also see a linear variation of phase, going through 2π radians in one wavelength. So we may be curious how the variation in phase along the bright ring compares to that in an ordinary traveling wave. We may ask what is the “effective wavelength” along the ring. We find

$$\lambda_r = \frac{x(n)}{n} \lambda_0$$

or

$$\lambda_r \approx \left(1 + \frac{2n + 1}{n(n + 3)}\right) \lambda_0$$

So the “wavelength” λ_r along the ring is somewhat longer than the “natural wavelength” λ_0 , particularly for small n .

This suggests that the phase shift variations in the “traveling wave” along an elongated pattern may need to be “slower” than expected, and that the “slowness” needs to be more pronounced for shorter features. We see later that the stretching of the apparent wavelength occurs with other elongated patterns and that the difference between the apparent and the underlying wavelength shrinks as the length of the pattern increases.

The total phase change expected with a normal traveling wave would have been $2\pi x(n)$ instead of $2\pi n$. The difference is

$$2\pi \frac{2n + 1}{n + 3}$$

Narrow Rectangle

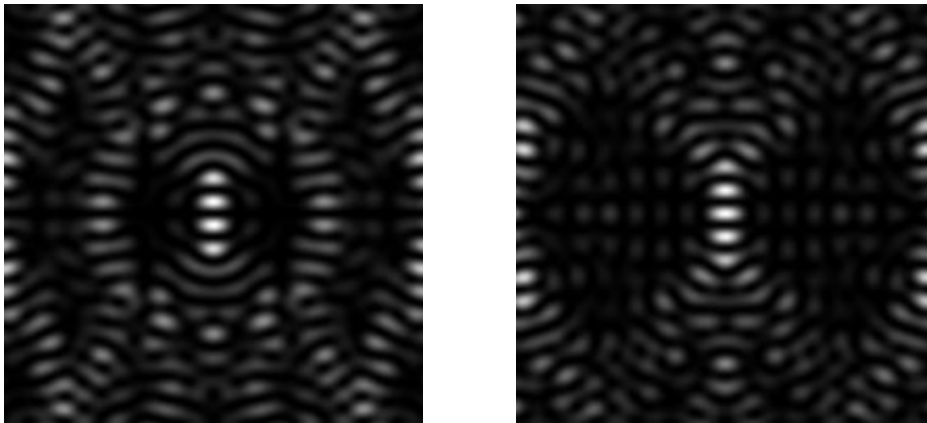
A point of light is useful, because, given enough time, any shape can be drawn with it. This is a slow process however. Pattern generation can be speeded up if larger sub-patterns can be generated. Presently most tools for generating semiconductor wafer patterns are restricted to combinations of rectangular areas. So it would be useful to find out first whether it is possible to create rectangular patterns, particularly narrow rectangular patterns that could be used for sections of lines.

Standing Wave Patterns

When beams with opposite wavenumber interfere, a standing wave pattern is produced with distance between peaks of $\lambda_0/2$. So it would appear

that it is may be possible to make patterns that consist of bright spots separated by about that distance. One could then use two exposures, one with the pattern displaced by $\lambda_0/4$ with respect to the other in order to fill in a line or narrow rectangular area.

Numerical experiments confirm this intuition. But the “double exposure” takes time, so an obvious next question is whether it is necessary for a pattern to have such rapid fluctuations in amplitude or whether it is possible to create patterns that have more or less constant amplitude along some extended feature. The answer is not obvious, since individual pairwise interference patterns have rapid fluctuations in one direction (while being constant in another).



Numerical Optimization Methods

We can approach this problem as one of determining the set of complex amplitudes for the beams that creates a pattern that is as close as possible to a given pattern in a least-squares sense. We can, for example, set up a regular grid of points on which the desired brightness is specified, and define as error terms the differences between the desired and the predicted brightness at each grid point.

A number of issues arise when considering this approach, including:

- (i) how to lay out the pattern of sample points;
- (ii) how finely to sample;
- (iii) how large a region to sample;
- (iv) what error function to use; and
- (v) what optimization method to use.

While layouts with hexagonal cells may provide advantages in terms of the degree of constraint provided by a given number of sample points, the simplicity of a square arrangement may make the latter the common

choice. There may be some effects that depend on alignment of the grid with the elongation of the desired brightness pattern. Irregular patterns may have some advantages in avoiding interactions between pattern orientation and the orientation of the sample layout.

The finer we sample, the more constraint we provide. At the same time, the number of components of the error vector grows quadratically with the fineness of the sampling grid. The brightness pattern we are sampling is band-limited to frequencies of no more than $2\omega_0$ and so the sampling theorem tells us that it can be sampled with a uniform grid with spacing $\pi/(2\omega_0) = \lambda_0/4$ between samples without losing information.

If samples are spaced more widely, the brightness pattern may take on unexpected values in between samples. For example, with a spacing of $\lambda_0/2$, standing waves with peaks on the grid points may occur, satisfying the constraints on the grid-points, yet dropping to low values in between.

We expect that there will be artifacts due to the fact that there are only a finite number of beams. These occur at some distance from strong parts of the pattern, experimentally determined to be round about

$$r_a \approx \frac{N}{2\pi} \lambda_0$$

The grid on which the desired pattern is defined should go out to about that distance to force the largest possible area of low brightness around the desired pattern. It probably makes little sense to go further since artifacts will occur beyond that that cannot be suppressed in any case.

The simplest measure of error would be the sum of squares of differences at each point of the grid between the desired pattern brightness and the brightness of the interference pattern computed from the set of complex amplitudes. The contributions may be weighted, by, for example, assigning low weights to “no care” positions on the grid.

Also note that typically numerical optimization methods work better when they are given an error vector rather than just the overall sum of squares of errors. In the simplest form, only the brightness is constrained. The real and imaginary parts of the complex amplitude are not dealt with separately, only the sum of their squares is compared with the desired brightness. If somehow the real and imaginary parts were known, double the number of constraints would be available to guide the numerical optimization. Interestingly, in areas where the desired brightness is zero, this observation can be exploited since both the real and the imaginary part of the complex amplitude should be zero.

Least squares minimization problems with complex relationships between the unknown variables to be determined and the error function tend

to be hard to deal with. Fortunately, ready-made packages are available. The modified Levenberg-Marquardt method is available in the “lmdif” subroutine of the MINPACK package. This employs a Jacobian calculated by a forward-difference approximation. This code was used for some of the numerical optimizations experiments described here.

For simpler error functions, simple methods like gradient descent will do. This happens, for example, when we specify the complex amplitude of the desired pattern rather than just the brightness at each sample point. We will see that this additional constraint is available if we make some additional assumptions.

Numerical Optimization Results

Naive numerical optimization for a rectangular brightness pattern, with large enough grid spacing, can lead to standing wave patterns that fit the desired pattern on the grid points, but have low values in between grid points. Such patterns can be used in pairs, one shifted $\lambda_0/4$ with respect to the other in order to approximate the desired rectangular shape.

With fine grid spacing the numerical optimization methods struggle and rarely produce reasonable solutions since they can’t resort to the standing wave “trick.”

The discussion earlier of travelling wave effects suggests that better results may be obtained by explicitly picking the phase of the desired pattern as well as the amplitude. The phase can be picked using an apparent wavelength somewhat longer than λ_0 in line with the discussion earlier of the phase variations along the bright ring.

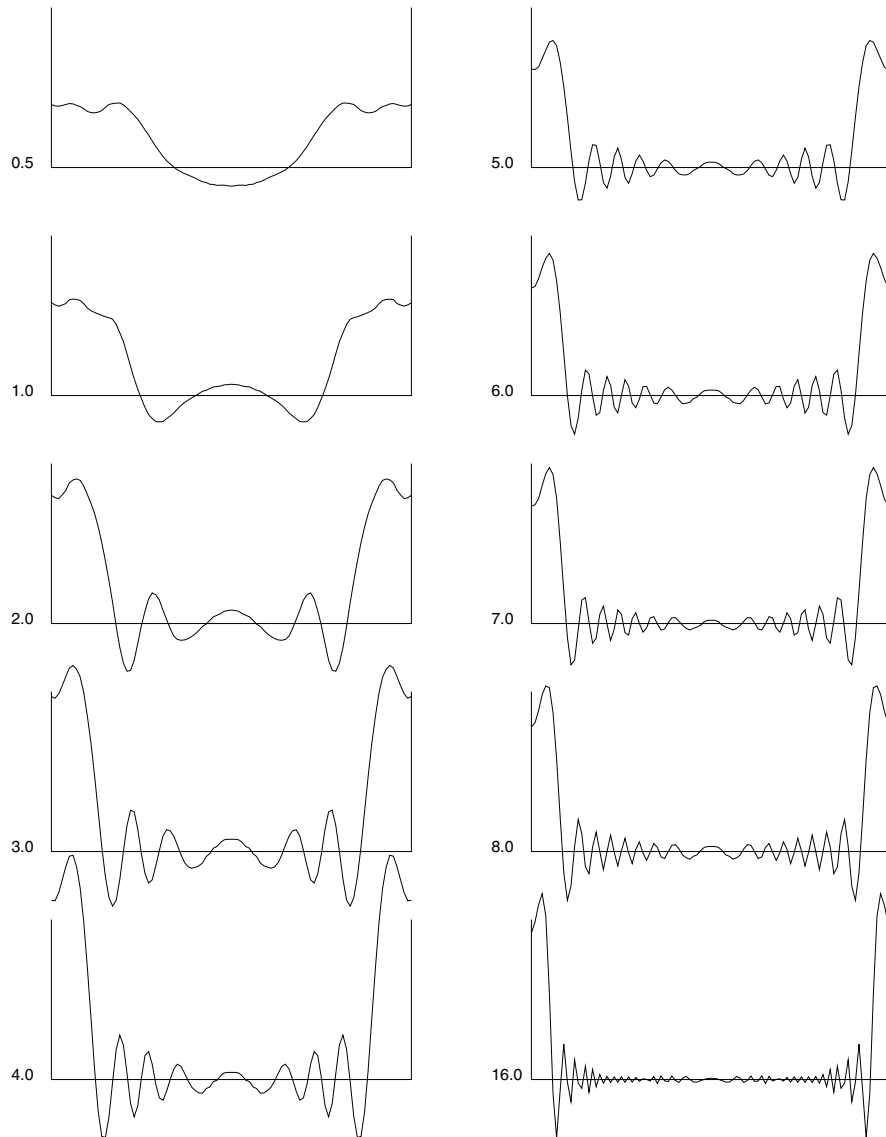
This indeed allows numerical optimization to produce interesting results. The quality of the results tends to depend on the “slowness” chosen for the travelling wave, that is, the ratio of the apparent wavelength to λ_0 . For short features, the wavelength should be considerably longer than λ_0 , while for long features it needs to be closer to λ_0 in value.

In this fashion reasonable approximations to small rectangular features were obtained. It is interesting to look at what the distribution of amplitudes of the beams is in such solutions. The solution typically has high amplitudes near one side of the ring, with lower amplitudes around the rest of it. The “standing wave” is produced predominantly by a few beams of high amplitude, with the other beams apparently mostly acting to destructively interfere with the main beams in areas where the desired pattern is zero.

These beam amplitude distributions when plotted against the angle of the beam direction look a little like decaying sinusoids, or rather like

“sinc” functions, but with variable sampling (that is, the spacing between successive zeros is not constant). The next figure shows such amplitude patterns for rectangular patterns of lengths equal to different multiples of λ_0 . Note that the waveform wraps around at the ends and that there are always two peaks, one on either side of the direction of the length of the rectangular pattern.

We see below that these amplitude waveforms are in fact samples along a circle in two dimensional space of a function that varies as the “sinc” of one of the coordinates.



Frequency Content of Rectangle

A rectangle centered at the origin with width a and height b can be treated as the convolution of a rectangular pulse along the x -axis of length a and a rectangular pulse along the y -axis of length b . Correspondingly, the Fourier transform is the product of the transforms of these two functions

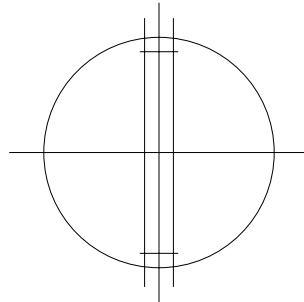
$$R(u, v) = ab \frac{\sin(ua/2)}{(ua/2)} \frac{\sin(vb/2)}{(vb/2)}$$

where (u, v) is the frequency.

This function has the first zero in the u direction at $\pm 2\pi/a$ and in the v direction at $\pm 2\pi/b$. The Fourier transform is zero along the edge of the rectangle defined by these values. While the transform has non-zero values outside the rectangle, most of the energy is inside it.

Let us assume that the long dimension of the original rectangle in the spatial domain is along the x -axis (i.e. $a \gg b$). Then the rectangle defined above in the frequency domain is narrow along the u axis and wide in the v direction since $2\pi/a \ll 2\pi/b$.

Now consider that we are restricted to generating frequency components along just a ring. We want to get the brightness pattern we generated to provide the best fit to the desired rectangle in the spatial domain. Fourier series have the interesting property that the best coefficients for a truncated series are in fact the first few coefficients of the full series. Similarly, the best complex amplitudes to assign along the ring — assuming that we are confined to using only Fourier components along that ring — are just the samples of the Fourier transform $R(u, v)$ along the ring.



In the figure, the circle is the ring on which the transform is sampled, while the vertical rectangle is where the transform of the narrow rectangular pattern is zero. Most of the energy of the “double sinc” function is inside this rectangle and it is clear that the ring samples outside this area.

If the length a of the rectangle is longer than the wavelength λ_0 , then $2\pi/a < \omega_0$. So the ring passes mostly *outside* the rectangle that contains most of the energy of the transform of the rectangle.

If the width of the rectangle b is small compared to the wavelength, then at least $2\pi/b > \omega_0$. In this case, the ring will pick up some part of the desired transform near $\nu \approx \pm\omega_0$ on and near the ν axis. The approximation will nevertheless be poor, even in this case, since most of the low frequency components are *not* sampled by the ring.

Shift in Frequency Domain

Things would be better if we could move the rectangle to a place where the ring intersects more of the area where the large values occur. So what does a shift in the frequency domain correspond to? Shifting the transform by (u_0, ν_0) in the transform domain only changes the phase of the spatial pattern, as can be seen easily from the formula for the inverse Fourier transform. At (x, y) the complex amplitude is simply multiplied by

$$e^{j(u_0x + \nu_0y)}$$

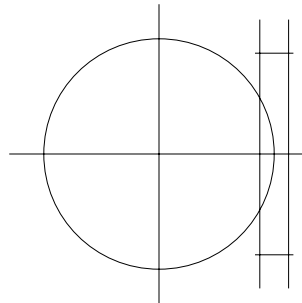
Brightness does not depend on the phase, so we do not care about the phase of the pattern we are creating. Consequently we can freely choose the phases of different parts of the pattern as desired.

In the case here, we would want to shift the rectangle in the transform domain in the u direction until much of it overlaps the ring on which we are allowed to have non-zero frequency components.

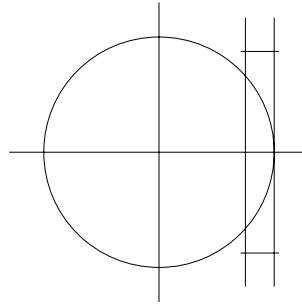
How Much to Shift

One remaining question is just how much to shift the transform:

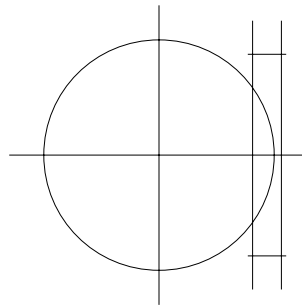
- (i) We could shift the rectangle so its center lies on the ring, that is by ω_0 . But this may not be optimal, since the ring then curves through the rectangle exiting on the left, leaving the right-hand side of the rectangle unsampled.



- (ii) Another idea might be to bring the rectangle just far enough out so its outer edge is tangent to the ring, that is, shift it by $\omega_0 - 2\pi/a$. But this also may not be optimal either, since then the highest part of the “double sinc” pattern lies inside the ring and is not sampled.

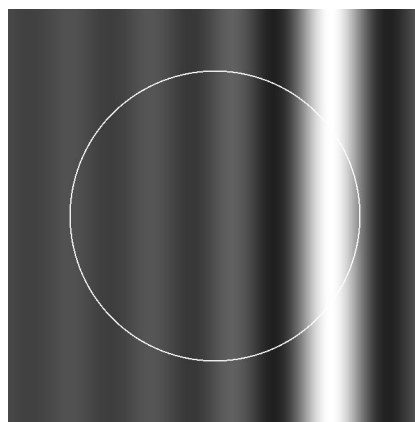


- (iii) A compromise would move the rectangle mid-way between the first two suggestions, that is by $\omega_0 - \pi/a$. Numerical experiments show that this is a near optimal compromise.

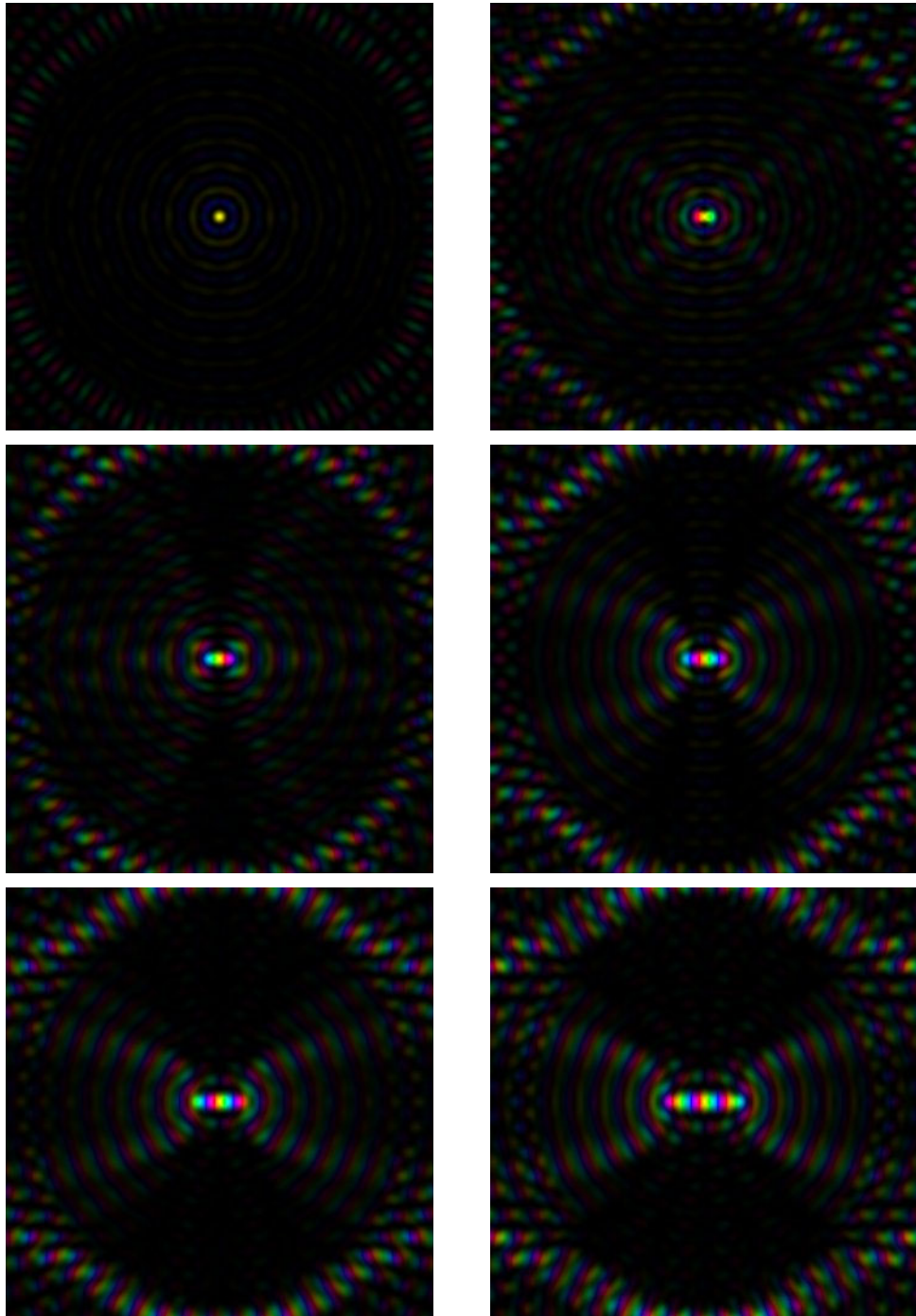


Note how the shift is substantially less than ω_0 when the rectangle is short, but approaches ω_0 as the rectangle becomes longer and longer.

This confirms the “slowed waves” intuition inspired by the circular ring pattern analysed earlier. The apparent wavelength of the travelling wave is longer than λ_0 , but gets smaller, and approaches λ_0 , as the elongated pattern gets longer.



The figure above shows how the circle samples a “sinc” function of u (the wider “sinc” function of v being omitted for clarity).



In the figures, brightness indicates amplitude, while color indicates phase. Shown are the approximate rectangular patterns generated of length $L = 0, 0.5, 1.0, 1.5, 2.0, 3.0 \lambda_0$. Note (i) “ghost” artifacts near the rectangle due to use of wavenumbers that lie on a circle in frequency space, (ii) artifacts in the outer areas due to the use of a finite number of beams.

Width of the Rectangle

A side-effect of the shift of the rectangle in the u direction in the transform domain is that some other areas of the transform of the rectangle are no longer sampled well. Before the shift, areas near the v -axis would be sampled out to $v = \pm\omega_0$. With the shift, the curvature of the ring causes it to depart from the areas directly above the center of the rectangle.

Suppose that we shift by $\omega_0 - \alpha(2\pi/a)$, with $0 \leq \alpha \leq 1$. Then the left edge of the rectangle lies at $\omega_0 - (\alpha + 1)2\pi/a$. The circle of radius ω_0 intersects this line at

$$v = \pm\sqrt{\omega_0^2 - \left(\omega_0 - (\alpha + 1)\frac{2\pi}{a}\right)^2}$$

or

$$v = \pm\sqrt{(\alpha + 1)\frac{2\pi}{a}}\sqrt{2\omega_0 - (\alpha + 1)\frac{2\pi}{a}}$$

Since this in effect limits the high frequency content in the y direction, we can expect that the actual shape created cannot be arbitrarily thin in that direction.

If we match this cut-off with the first zero of the sinc function we see that the “equivalent thickness” b' of the resulting shape is determined by $2\pi/b' = v$. Now $\omega_0 \gg (\alpha + 1)2\pi/a$ when $a \gg (\alpha + 1)\lambda_0$, so

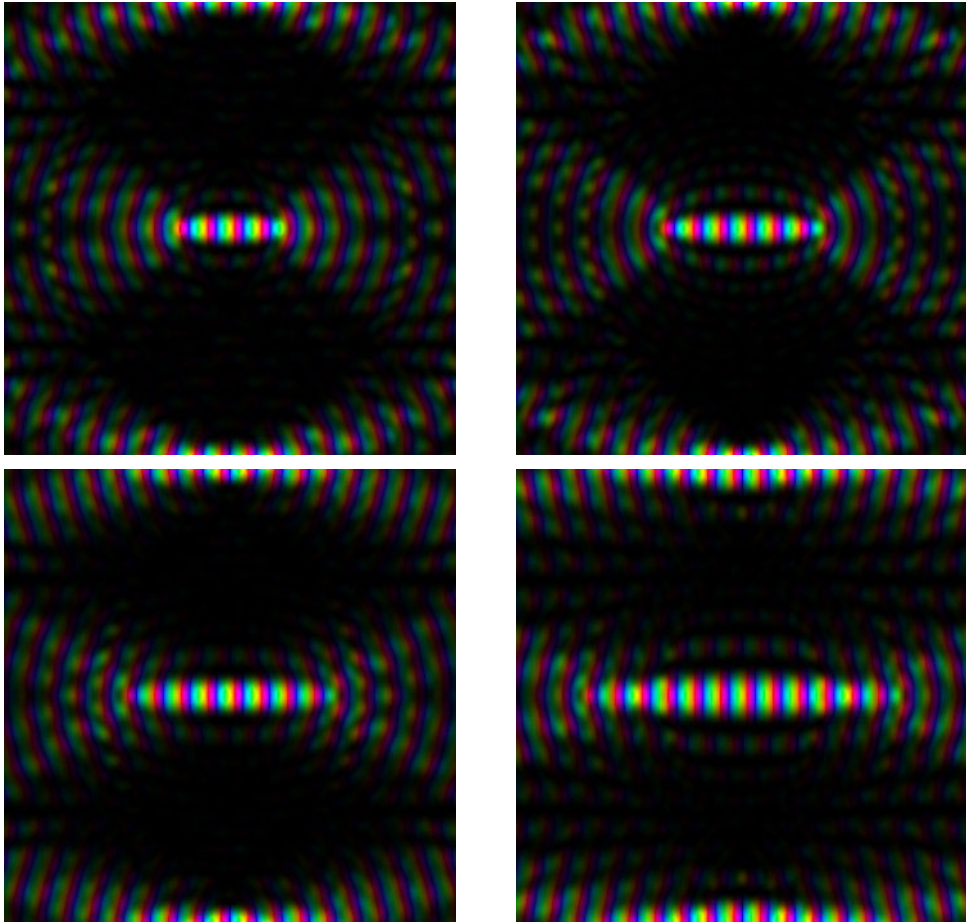
$$v \approx 2\pi\sqrt{\frac{2(\alpha + 1)}{a\lambda_0}}$$

and

$$b' \approx \sqrt{\frac{a\lambda_0}{2(\alpha + 1)}}$$

That is, the width of the approximate rectangular feature we can generate grows as the square root of its length. This is born out by numerical experiments.

So, while, for speed, we would like to be able to make very long linear features, the fact is that when we make them long, they also get wider. Consequently very long thin patterns will have to be printed in sections. Note that what is considered “long” is here determined by how long it is in relation to the wavelength λ_0 .



This figure shows approximately rectangular patterns of length $L = 4, 6, 8,$ and $12 \lambda_0$ generated by the method described. Note how (i) the longer shapes are wider (but not in direct proportion to the length), (ii) the shapes tend to be somewhat rounded and thinner at the ends, and (iii) artifacts are more prominent near the ends.

Nature of Artifacts

There are two types of artifacts:

- (i) artifacts that arise because we can only use spatial frequencies that lie on a circle in the transform domain;
- (ii) artifacts that arise because we only have a finite number of beams.

Typically artifacts of the latter type appear at a distance of about

$$r_a \approx \frac{N}{2\pi} \lambda_0$$

from strong pattern features.

So, if the pattern is a point at the origin, then few serious artifacts appear closer to the origin than the “ring of artifacts” at about r_a . If the pattern is more complex, with parts of it away from the origin, then some artifacts will correspondingly be closer to the origin.

Clearly, however, the latter type of artifacts can be pushed outward by increasing the number of beams.

Summary

The exploration of numerical and analytical approaches to the problem of discovering complex beam amplitude patterns to produce desired interference patterns has led to some useful insights:

- (i) Elongated patterns with constant amplitude can be made if the phase is allowed to vary linearly along the pattern.
- (ii) The variation of phase along the elongated feature is slower than that along an ordinary travelling wave. That is, the “equivalent wavelength” is longer than the effective wavelength λ_0 of light on the reference surface.
- (iii) The difference in wavelengths is less pronounced for longer features.
- (iv) For long features, only a few of the beams on one side of the ring are being used at high power.
- (v) The width of elongated patterns that can be generated this way is proportional to the geometric mean of the length and the wavelength of light.
- (vi) Numerical optimization is drastically simplified if both amplitude and phase are specified for the desired pattern. We need to come up with an intelligent guess at what a good phase distribution might be.

It is expected that additional improvements in the generated patterns may be possible by allowing numerical optimization to adjust the desired phases along the pattern, starting from the guess obtained by assuming a fixed predefined equivalent wavelength for the travelling wave.

References

- [1] Mermelstein, Michael S. “Synthetic Aperture Microscopy,” Ph.D. Thesis, MIT EECS, June 1999.